Noise-induced transitions in human postural sway

Christian W. Eurich and John G. Milton*
Department of Neurology and Committee on Neurobiology, The University of Chicago, MC 2030, 5841 South Maryland Avenue, Chicago, Illinois 60637
(Received 8 July 1996)

Correlation functions with multiple scaling regions occur in the description of the fluctuations in the center of pressure during quiet standing. Postural sway is modeled as an inverted pendulum with a delayed feedback constructed such that for deviations beyond a spatial threshold a constant restoring force is engaged. In the absence of noise, two stable limit cycles coexist. The correlation function depends on the added noise intensity: at intermediate noise levels three scaling regions appear whereas only two occur for high noise levels. Our observations suggest that correlation functions with multiple scaling regions reflect noise-induced transitions in bistable dynamical systems. [S1063-651X(96)00112-2]

PACS number(s): 87.10.+e, 05.40.+j, 02.30.Ks

The human nervous system operates in a very noisy environment and hence noise-induced transitions are likely to play a major role in shaping its dynamics [1,2]. In multistable dynamical systems noise can induce transitions between different attractors [2,3]. Multistability readily arises in mathematical models with time-delayed feedback [4], including those which describe neural control mechanisms [5], and has been observed experimentally in neural circuits constructed from invertebrate neurons [6], in model electronic circuits [7], and in optical dye laser experiments [8]. Here we draw attention to the observation that noise-induced transitions in multistable dynamical systems can lead to correlation functions characterized by the presence of multiple scaling regions.

To illustrate our findings we examine the fluctuations which occur in the center of pressure (COP) during quiet standing [9–11]. These dynamics are not chaotic, but are indistinguishable from correlated noise and can be modeled as bounded, correlated random walks [10,12]. The two-point correlation function measured in either the back to front or side to side direction, x, $K(\Delta t)=\langle[x(t)-x(t+\Delta t)]^2\rangle$, where the brackets indicate a time average along a single trajectory and Δt is the time increment [9,13], typically contains three regions (Fig. 1). Since for a correlated random walk we have the scaling law $\langle K(\Delta t)\rangle\sim\Delta t^{2H}$, where $0<H<1$ is a scaling exponent [14], this observation suggests the presence of multiple scaling regions [9–11].

We model human postural sway by the movement of an inverted pendulum which is subjected to both noisy perturbations and a time-delayed restoring force [15], i.e.,

$$mR^2\ddot{\phi}+\gamma\dot{\phi}-mgR\,\sin\phi=\tilde{f}(\phi(t-\tau'))+\sqrt{2\tilde{d}}\xi(t), \quad (1)$$

where m is the mass (center of mass located at a distance R from the ground), g is the gravitational constant, γ is the damping coefficient, ϕ is the tilt angle ($\phi=0$ corresponds to the upright position, hence the ''$-$'' sign), and $\sqrt{2\tilde{d}}\xi(t)$ is δ-correlated Gaussian noise of intensity $\sqrt{2\tilde{d}}$. Once a displacement occurs, the application of the restoring force is delayed by a time τ' as a consequence of finite neural conduction and processing times and neuromuscular response times [12,16]. Since postural sway control mechanisms are overdamped for healthy subjects with eyes open [11,17], $\gamma\dot{\phi}\gg mR^2\ddot{\phi}$, we can rewrite (1) for small displacements in the x direction as

$$\dot{x}=\alpha x+\sqrt{2d}\xi(t)+f(x(t-\tau')), \quad (2)$$

where $\alpha=mgR/\gamma>0$ is a rate constant, $x=R\sin\phi$, and d,f are the rescaled $\tilde{d},\tilde{f}$.

During postural sway movement occurs primarily at the ankle joint. Information concerning joint position is detected by threshold-type sensory neurons, i.e., the neurons only become activated once joint angle exceeds a certain value [18]. Thus the postural sway feedback f operates by allowing the system to drift for small displacements (open loop control) with stabilizing negative feedback (closed loop control) only becoming significant for sufficiently large displacements (times) [9,10,12]. A possible choice of f which is consistent with these observations can be constructed from sigmoids of the form $f(x)=1/(1+e^{-\beta x})$. Figure 2 plots $\dot{x}$ versus x for

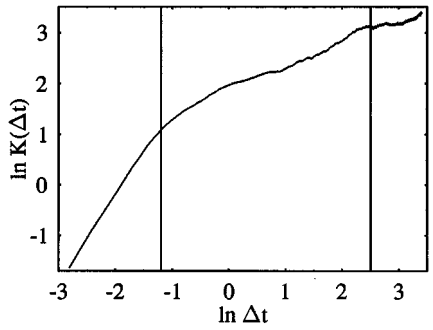

FIG. 1. Plot of the COP two-point correlation function $K(\Delta t)$ versus time interval Δt for a healthy 21 year old female (height 1.63 m, weight 63.5 kg). Vertical lines segment $K(\Delta t)$ into different scaling regions: (from left to right), $H\sim0.86$, $H\sim0.29$, $H\sim0$ [11].

*Author to whom correspondence should be addressed.

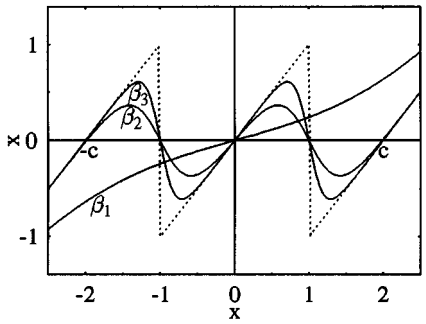

FIG. 2. Plot of $\dot{x}$ versus x for (6) as a function of β (proportional to the gain) in the feedback control described by (3) (solid line). A piecewise linear approximation used in (6) is represented by the dotted line. $c=2$, $\theta=1$, $\beta_1=1$, $\beta_2=5$, $\beta_3=10$.

$$f(x)=c\left\{1-\frac{1}{1+e^{-\beta(x-\theta)}}-\frac{1}{1+e^{-\beta(x+\theta)}}\right\}, \tag{3}$$

where c,θ are constants for different values of β. For small displacements from the vertical the restoring force is small (''open loop control''), for larger displacements the restoring force stabilizes the upright position (''closed loop control''), and for sufficiently large displacements the restoring force is incapable of stabilizing the upright position and the swayer topples over.

Joint position receptors typically discharge maximally within a very small range of angles [19]. For large β we approximate f by the piecewise constant approximation (dotted line in Fig. 2), i.e.,

$$f=\begin{cases} 0 & \text{if } x\leqslant\theta \\ -c & \text{if } x>\theta. \end{cases} \tag{4}$$

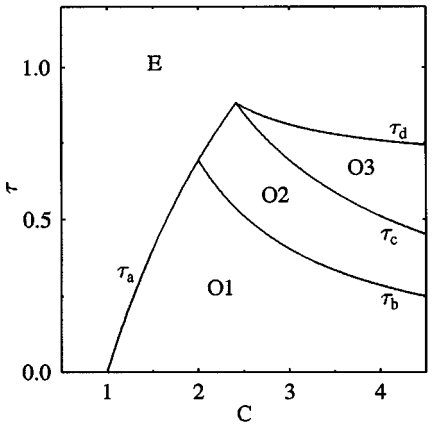

FIG. 3. Steady state behavior of (6) in the absence of noise. Oscillations of the type shown in Fig. 4 top occur for choices of C and τ in the region labeled ''$O1$''; of the type in Fig. 4 middle in the region labeled ''$O2$,'' and of the type shown in Fig. 4 bottom in the region labeled ''$O3$.'' There are also different kinds of unstable solutions (the swayer falls) which are designated as E in the bifurcation diagram and are not discussed further.

After rescaling x and t, (2) reduces to

$$\dot{x}=\begin{cases} x+\sqrt{2D}\xi(t)+C & \text{if } x(t-\tau)<-1 \\ x+\sqrt{2D}\xi(t) & \text{if } -1\leqslant x(t-\tau)\leqslant 1 \\ x+\sqrt{2D}\xi(t)-C & \text{if } x(t-\tau)>1, \end{cases} \tag{5}$$

where $\tau=\alpha\tau'$, $C=c/\alpha\theta$, and $D=d/\alpha^2\theta^2$.

In the absence of noise, $D=0$, the solution of (5) is

$$x(t)=\begin{cases} -C+[x(t_0)+C]\exp(t-t_0) & \text{if } x(t-\tau)<-1 \\ x(t_0)\exp(t-t_0) & \text{if } -1\leqslant x(t-\tau)\leqslant 1 \\ C+[x(t_0)-C]\exp(t-t_0) & \text{if } x(t-\tau)>1. \end{cases} \tag{6}$$

The dynamics of (5) can be readily determined from (6) with the help of Fig. 2. In the following, we take initial conditions $|x(s)|\leqslant 1$, $s\in[-\tau,0]$.

Figure 3 shows the bifurcation diagram of (5). No stable fixed point solutions can occur (Fig. 2). However, three different stable limit cycle solutions arise, denoted by $O1,O2,O3$ (Figs. 3, 4) [20]. Bounded solutions occur only for $C\geqslant 1$; otherwise, $\dot{x}>0$ for $x>0$ and $\dot{x}<0$ for $x<0$, which results in an immediate escape for almost all initial conditions. The region in the parameter space where bounded solutions exist is specified by two conditions. First, let $x(t_0)=1$ and $0\leqslant x(s)\leqslant 1$ for $s\in[t_0-\tau,t_0]$; then for a solution to have an upper boundary, we must have $x\leqslant C$ at $t=\tau$, i.e.,

$$\tau\leqslant\tau_a(C)\equiv\ln(C) \tag{7}$$

(see Fig. 3). Second, in order to obtain a condition for the solution to have a lower boundary, let $x(t_0)=1$ and $1\leqslant x(s)\leqslant C$ for $s\in[t_0-\tau,t_0]$. Assume further that at time $t_1:=t_0+\tau$, $-C\leqslant x\leqslant -1$. Then there exists a time $t^*\in[t_0,t_1]$ such that $-1\leqslant x(s)\leqslant 1$ for $s\in[t_0,t^*]$. The requirement that $x(t)\geqslant -C$ at time $t^*+\tau$ leads to the condition

$$\tau\leqslant\tau_d\equiv\ln\frac{2C^2}{C^2-1} \tag{8}$$

(see Fig. 3). Due to the symmetry of (5), the same conditions arise if $x(t_0)=-1$.

The stable limit cycle $O1$ (Fig. 4 top) encircles $+1$ with $x>0$ for all time [21]. From (5) it can be seen that $O1$ occurs when C, τ satisfy (Fig. 3)

$$\tau<\tau_a(C) \quad \text{and} \quad 0<\tau<\tau_b(C)\equiv\ln\frac{C}{C-1}. \tag{9}$$

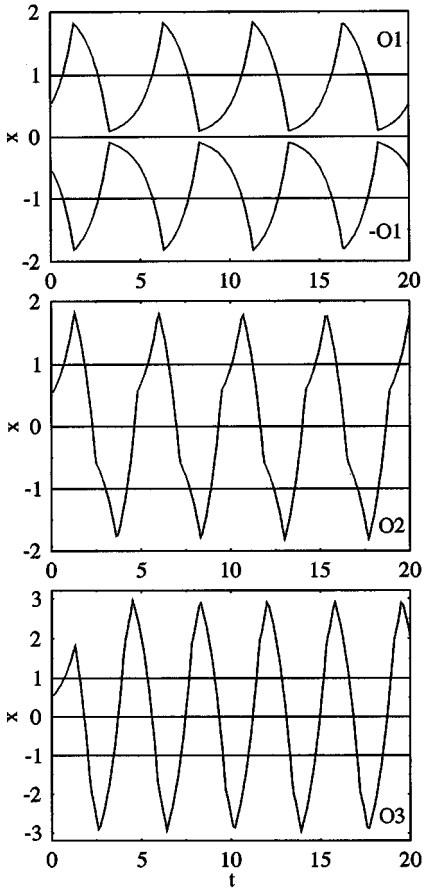

FIG. 4. Three types of oscillations predicted by (5). In all cases $\tau=0.6$. Values for C are top, $C=-2.1$; middle, $C=2.9$; bottom, $C=4.5$.

This limit cycle coexists with another $(-O1)$ that encircles -1 with $x<0$ for all time. Thus we have bistability; the solution which is observed depends on the choice of the initial condition.

The system shows two more qualitatively different limit cycles, $O2$ and $O3$, each of which enclose ± 1 (Figs. 4 middle and bottom). The conditions for $O2$ and $O3$ to occur are, respectively,

$$\tau<\tau_a(C) \quad \text{and} \quad \tau_b(C)<\tau<\tau_c(C)\equiv \ln\frac{C+1}{C-1} \tag{10}$$

and

$$\tau_c(C)<\tau<\tau_d(C) \tag{11}$$

(Fig. 3). Bistability arises also in these cases. However, the coexisting orbits ($-O2$ and $-O3$) are identical in shape to, respectively, $O2$ and $O3$; they differ only by a phase shift. We do not consider $O2$ and $O3$ further. By comparing (7) and (8) to (9)–(11) it is clear that no other solutions, e.g., chaotic trajectories, can arise in (5).

When C, τ correspond to cases in which the limit cycles $O1$ and $-O1$ coexist, noise can induce transitions between two qualitatively different attractors. Figure 5 shows the two-point correlation function $K(\Delta t)$ as a function of the noise intensity D. For low noise levels, $K(\Delta t)$ shows oscillations.

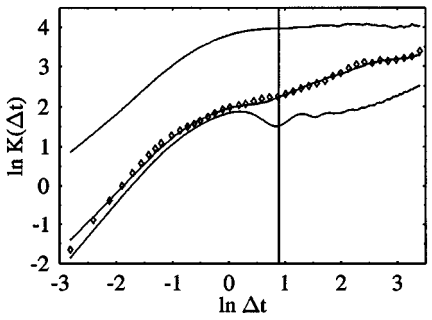

FIG. 5. Two-point correlation functions of the unscaled version of (5) for different values of noise intensity. Top: $d=0.166$ mm^2 sec^{-2}; middle: $d=0.625$ mm^2 sec^{-2}; bottom: $d=1.020$ mm^2 sec^{-2}. In all cases, $\alpha=0.60$ sec^{-1}, $\theta=5.95$ mm, $c=19.67$ mm sec^{-1}, $\tau'=233$ msec. Diamonds show experimental data taken from Fig. 1.

For intermediate noise levels, $K(\Delta t)$ contains three regions and is identical to that observed experimentally. From the model we obtain $\tau'\sim 230$ msec and $\theta\sim 6$ mm, which agree remarkably well with those values observed experimentally, respectively, 200–300 msec [16] and 5–6 mm [18]. Finally, as the noise intensity increases the three regions become less distinct and finally disappear at high noise levels.

We conjecture that there are two essential features to produce a correlation function with multiple scaling regions: (1) two or more coexisting limit cycle attractors in which transitions between attractors occur only at certain phases of the cycle (e.g., minimum of $O1$ in Fig. 4 top); and (2) noise of sufficient intensity to cause transitions between the attractors at not too high a rate. The vertical line in Fig. 5 shows that the break between the first two scaling regions in $K(\Delta t)$ occurs just before the period of the oscillation for the noiseless case. For Δt shorter than one period of the limit cycle, transitions occur only in one direction between basins of attraction, e.g., $1\rightarrow 2$. These transitions are reflected by an increase in $K(\Delta t)$. For Δt longer than the period of the limit cycle, transitions of the form $1\rightarrow 2\rightarrow 1$ begin to occur and $K(\Delta t)$ increases less rapidly. Finally for long Δt, it becomes equally probable that the swayer is in either basin of attraction and $K(\Delta t)$ reflects the mean displacement.

To test this hypothesis we studied the Mackey-Glass equation [24] with an additive noise input

$$\dot{x}=-ax+\frac{bx(t-\tau)}{1+x(t-\tau)^n}+\sqrt{2d}\,\xi(t), \tag{12}$$

where a,b,n are positive constants. When n is even and $d=0$, this equation is invariant under the transformation $x(t)\rightarrow -x(t)$ and hence there is bistability [7]: if $x(t)$ is a limit cycle solution of (12) then so is $-x(t)$. Numerical simulations indicate that the two-point correlation for this system exhibits qualitatively the same behavior as our model for postural sway (data not shown).

Experimentally the situation with three scaling regions is most often seen [9–11]; however, for some subjects three regions are less apparent and for others oscillations occur [12]. Here we have shown that the shape of $K(\Delta t)$ depends

on three parameters: the time delay τ, the strength of the feedback C, and the noise intensity D [22]. From Fig. 3 it is clear that it should be possible to change the shape of $K(\Delta t)$ by altering these parameters, e.g., drinking alcohol to alter τ [23]; holding a weight over the head to raise the center of gravity to alter α and hence τ, C, D; adding noisy perturbations to the pressure platform to alter D.

The study of noise-induced transitions in stochastic delay differential equations has only begun to receive attention [3]. A variety of routes and mechanisms for noise-induced transitions can occur. Moreover, transitions can involve new states created by the addition of noise to the system [25], i.e., states which were not present in the absence of noise. Thus it is possible that $K(\Delta t)$ can have a shape which is more complex than we have considered here. Our results should alert the experimentalist to the possible connection between a correlation function with multiple scaling regions to an underlying multistable dynamical system in which noise-induced transitions are occurring.

We thank J. Collins, R. E. Jaeger, M. C. Mackey, and T. Ohira for useful discussions. C.W.E. was supported by BASF. Research was supported by grants from the National Institutes of Mental Health and the Brain Research Foundation. Experimental data for Fig. 1 were supplied by and published with the permission of J. Collins.

[1] J. Rinzel and S. M. Baer, Biophys. J. **54**, 551 (1988); S. M. Baer, T. Erneux, and J. Rinzel, SIAM J. Appl. Math. **49**, 55 (1989); A. Longtin, J. G. Milton, J. E. Bos, and M. C. Mackey, Phys. Rev. A **41**, 6992 (1990); A. Longtin, *ibid*. **44**, 4801 (1991); M. C. Mackey and I. Nechaeva, Phys. Rev. E **52**, 3366 (1995).

[2] A. Longtin, A. Bulsara, and F. Moss, Phys. Rev. Lett. **67**, 656 (1991); F. Moss, D. Pierson, and D. O'Gorman, Int. J. Bifurc. Chaos **4**, 1383 (1994).

[3] K. Kapral, E. Celarier, P. Mandel, and P. Nardone, SPIE Opt. Chaos **667**, 175 (1986); J. Foss, F. Moss, and J. Milton (unpublished).

[4] U. an der Heiden and M. C. Mackey, J. Math. Biol. **16**, 75 (1982); I. Ikeda and K. Matsumoto, Physica D **29**, 223 (1987).

[5] S. A. Campbell, J. Bélair, T. Ohira, and J. Milton, Chaos **5**, 640 (1995); J. Dyn. Diff. Eqs. **7**, 213 (1995); J. Foss, A. Longtin, B. Mensour, and J. Milton, Phys. Rev. Lett. **76**, 708 (1996).

[6] D. Kleinfeld, F. Raccuia-Behling, and H. J. Chief, Biophys. J. **57**, 697 (1990).

[7] J. Losson, M. C. Mackey, and A. Longtin, Chaos **3**, 167 (1993).

[8] T. Aida and P. Davis, IEEE J. Quantum Electron. **28**, 868 (1992).

[9] J. J. Collins and C. J. de Luca, Exp. Brain Res. **95**, 308 (1993); Chaos **5**, 57 (1995); Exp. Brain Res. **103**, 151 (1995).

[10] J. J. Collins and C. J. de Luca, Phys. Rev. Lett. **73**, 764 (1994).

[11] C. C. Chow and J. J. Collins, Phys. Rev. E **52**, 907 (1995).

[12] T. Ohira and J. G. Milton, Phys. Rev. E **52**, 3277 (1995). Three scaling regions can be observed when a threshold is added to a model for a delayed random walk [T. Ohira, Sony Computer Science Laboratory, Technical Report No. SCSL-TR-96-12, 1996 (unpublished)].

[13] The two-point correlation function used by Collins and coworkers is related to the autocorrelation, $\langle x(t)x(t+\Delta t)\rangle$, by the relation $\langle [x(t)-x(t+\Delta t)]^2\rangle = 2\langle x^2(t)\rangle - 2\langle x(t)x(t+\Delta t)\rangle$.

[14] B. B. Mandelbrot and J. W. van Ness, SIAM Rev. **10**, 422 (1968); J. Feder, Fractals (Plenum, New York, 1988).

[15] F. Schürer, Math. Nachr. **1**, 295 (1948); U. an der Heiden, J. Math. Biol. **8**, 345 (1979).

[16] M. H. Woolacott, C. von Hosten, and B. Rösblad, Exp. Brain Res. **72**, 593 (1988).

[17] S. A. S. Werness and D. J. Anderson, Biol. Cybern. **51**, 155 (1984).

[18] M. G. Gilsin, C. G. Van den Bosch, S-G. Lee, J. A. Ashton-Miller, N. B. Alexander, A. B. Schultz, and W. A. Ericson, Age Aging **24**, 58 (1995); C. G. Van den Bosch, M. G. Gilsing, S.-G. Lee, J. K. Richardson, and J. A. Ashton-Miller, Arch. Phys. Med. Rehabil. **76**, 850 (1995).

[19] P. Griggs and B. J. Greenspan, J. Neurophysiol. **40**, 1 (1977); *Handbook of Physiology, Volume 1: Excitable Cells and Neurophysiology*, edited by H. D. Patton, A. F. Fuchs, B. Hille, A. M. Scher, and R. Steiner (Saunders, Philadelphia, 1989).

[20] Bistability also exists for (2) when f is composed of smooth sigmoidal functions such as (3). The behavior depends on the value of β. For small β there is the coexistence of two stable fixed points. For sufficiently large β these fixed points become unstable and are replaced by stable limit cycles. Numerical simulations suggest that the dynamics which occur for large β are qualitatively similar to those predicted to occur from the piecewise constant approximation.

[21] The period of the oscillation is $T_1 = 2\tau + \ln\{(C-1)/(C-1)\exp(2\tau) + C^2[1-\exp(\tau)]\}$.

[22] Three scaling regions have been reproduced in a stochastically driven pinned polymer model for postural sway in which the stochastic forcing itself has a power-law scaling over short times [11].

[23] M. H. Woollacott, Exp. Neurol. **80**, 55 (1983).

[24] M. C. Mackey and L. Glass, Science **197**, 287 (1977).

[25] W. Horsthmenke and R. Lefever, *Noise-induced Transitions: Theory and Applications in Physics, Chemistry and Biology* (Springer-Verlag, New York, 1984); A. Lasota and M. C. Mackey, *Chaos, Fractals and Noise: Stochastic Aspects of Dynamical Systems* (Springer-Verlag, New York, 1994).